Scientific Research Publishing

Retraction Notice

Title of retracted article: **Energy Flux Distribution and Thermal Performance of Linear Fresnel Collector System in Cold Region**

Author(s): Jing Ma*, Zheng Chang, Rui Tian

* Corresponding author. Email: majing426520829@163.com

Journal: Energy and Power Engineering (EPE)
Year: 2017
Volume: 9
Number: 10
Pages (from - to): 555 - 567
DOI (to PDF): http://doi.org/10.4236/epe.2017.910039
Article page: http://www.scirp.org/Journal/PaperInformation.aspx?PaperID=79006

Retraction date: 2018-6-5

Retraction initiative (multiple responses allowed; mark with **X**):

X All authors
☐ Some of the authors:
☐ Editor with hints from
  O Journal owner (publisher)
  O Institution:
  O Reader:
  O Other:

Date initiative is launched: 2018-6-4

Retraction type (multiple responses allowed):

☐ Unreliable findings
  O Lab error O Inconsistent data O Analytical error O Biased interpretation
  O Other:
☐ Irreproducible results
☐ Failure to disclose a major competing interest likely to influence interpretations or recommendations
☐ Unethical research

☐ Fraud
  O Data fabrication O Fake publication O Other:
☐ Plagiarism ☐ Self plagiarism ☐ Overlap ☐ Redundant publication *
☐ Copyright infringement ☐ Other legal concern:

☐ Editorial reasons
  O Handling error O Unreliable review(s) O Decision error O Other:

X Other:

Results of publication (only one response allowed):

☐ are still valid.
X were found to be overall invalid.

Author's conduct (only one response allowed):

☐ honest error
☐ academic misconduct
X none (not applicable in this case – e.g. in case of editorial reasons)

* Also called duplicate or repetitive publication. Definition: "Publishing or attempting to publish substantially the same work more than once."

History
Expression of Concern:
☐ yes, date: yyyy-mm-dd
X no

Correction:
☐ yes, date: yyyy-mm-dd
X no

Comments:

Large-scale corrections should be made to the paper.

This article has been retracted to straighten the academic record. In making this decision the Editorial Board follows COPE's Retraction Guidelines. Aim is to promote the circulation of scientific research by offering an ideal research publication platform with due consideration of internationally accepted standards on publication ethics. The Editorial Board would like to extend its sincere apologies for any inconvenience this retraction may have caused.

Editor guiding this retraction: Dr. Fermin Mallor (EiC of EPE)

Scientific Research Publishing

Energy and Power Engineering, 2017, 9, 555-567
http://www.scirp.org/journal/epe
ISSN Online: 1947-3818
ISSN Print: 1949-243X

Energy Flux Distribution and Thermal Performance of Linear Fresnel Collector System in Cold Region

Jing Ma[1*], Zheng Chang[1], Suying Yan[1,2], Rui Tian[1,2]

[1]College of Energy and Power Engineering, Inner Mongolia University of Technology, Hohhot, China
[2]Key Laboratory of Wind and Solar Power Energy Utilization Technology Ministry of Education and Inner Mongolia Construction, Hohhot, China
Email: *majing426520829@163.com

How to cite this paper: Ma, J., Chang, Z., Yan, S.Y. and Tian, R. (2017) Energy Flux Distribution and Thermal Performance of Linear Fresnel Collector System in Cold Region. *Energy and Power Engineering*, **9**, 555-567.
https://doi.org/10.4236/epe.2017.910039

Received: July 31, 2017
Accepted: September 9, 2017
Published: September 12, 2017

RETRACTED

Abstract

In this paper, on the base of principle of linear Fresnel reflective collector, a three-dimensional framework of linear Fresnel reflector field (LFR), compound parabolic collector (CPC) and the absorber tube with selective absorption coating and glass tube were established, together with calculating optical efficiency of the vacuum tube collector at different incident angles of the linear Fresnel system in the cold region. As revealed by the findings, the angle of light was in the range of 0˚ - 60˚, and the optical efficiency amounted to be the lowest at the incident angle of 15˚. When the incident angle was 75˚, the optical efficiency displayed an obvious reduction, and as the incident angle was 0˚, the distribution of the energy flow in the tube was more standardized. Because of the incidence of the end loss, some tube length is unable to flow in the direction. For the purpose of performing the experiment the thermal performance of linear Fresnel system in the cold region, introduction of the thermal transfer factor was made, together with the analysis of the measured data under the condition of no loss of the receiver. The maximum theoretical efficiency of the system amounted to 68%, and the optical loss was approximately the total solar radiation at 32%.

Keywords

Linear Fresnel Collector, Cold Region, Instantaneous Thermal Efficiency, Energy Flux Density Distribution

1. Introduction

Linear Fresnel systems are among the most promising technologies used for energy generation from concentrated sun radiation. In such plants, a linear fixed receiver is suspended above a solar field which comprises strips of mirrors, flat or slightly concentrating; each strip rotates on a fixed horizontal axis for the purpose reflecting the sun radiation towards the receiver [1] [2]. Linear Fresnel [3] [4] solar concentrating heat collection system, for its own compact structure, ease of manufacture, low price and other associated benefits in the field of solar energy, is put to a widespread use. The arrangement of linear Fresnel mirror field poses an enormous impact on its optical efficiency as well as heat source temperature. Currently, local and international scholars have carried out the analysis of the arrangement of linear Fresnel mirror field. Moreover, measurement of the optical image was computed numerically. Several studies have been devoted to plant configurations study and simulation of various aspects of the plant work, comparisons with linear trough systems [5]. Abbas *et al.* [6] [7] proposed a new arrangement of the heat absorber. Furthermore, the linearity of the linear Fresnel internal mirror was modified and the optical efficiency of the linear Fresnel field was also enhanced. There are different LFC receiver technologies: cavity receivers with an array of parallel tubes [8] [9], utilized by Areva-Solar and among others, are included by Novatec Solar and Solarmundo [10], as well as single tube receiver with other geometries secondary reflector [11], Qiu *et al.* [12] [13] performed the study of the coupling heat transfer process of radiation-conduction-convection in LFR heat absorbers under non-uniform energy flux distribution boundary conditions, analyzed the photo-thermal conversion performance of the LFR system, in addition to obtaining the non-uniform temperature distribution of the surface of the absorber tube.

Focus has been thrown by earlier research studies on the arrangement and numerical measurement of linear Fresnel spectroscopy. Furthermore, there are a few analyses on the energy flux distribution of the absorber tube and the efficiency of the system heat collection in the cold region. For the purpose of performing accurate analysis on the influence of latitude for the receiver surface energy distribution of the linear Fresnel system, this paper, at first, made use of the TracePro software in order to model the linear Fresnel mirror field. It combined with the latitude of the cold region to change the solar elevation angle, and then analyzed the changes of the optical efficiency of the system subjected to varied angles of incidence. Contrast latitude 0˚ and latitude 40.8˚, the absorber tube circumferential and length direction energy density distribution changes, as well as the linear Fresnel experimental system were experimented, and the thermal transfer factor was introduced to perform the analysis of thermal efficiency of the system.

2. Optical Modeling of the Linear Fresnel Solar Field

2.1. Optical-Geometrical Model

In this paper, the linear Fresnel mirror field has been presented in **Figure 1(a)**, primarily by mirrors, CPC, glass-metal vacuum tube and tracking device. The

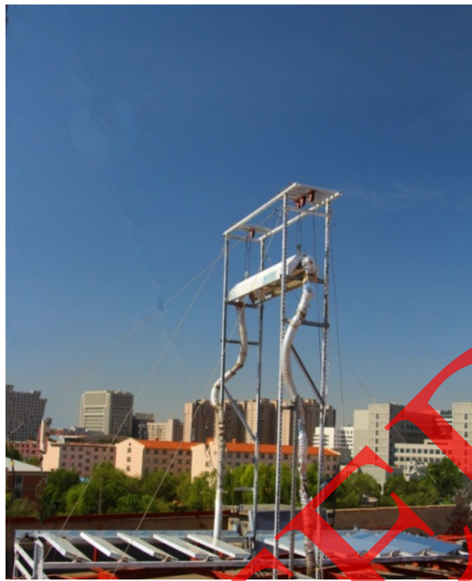

(a)

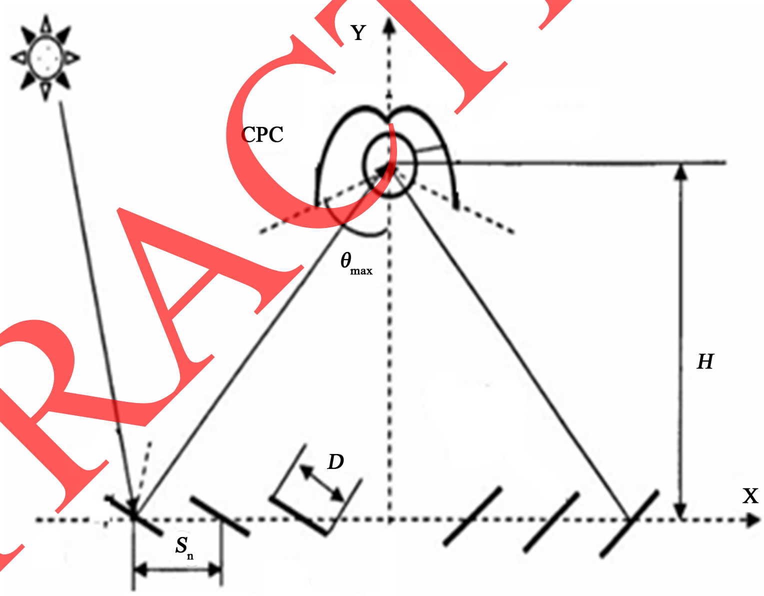

(b)

Figure 1. (a) Photo of the experimental linear Fresnel system; (b) Schematic diagram of a linear Fresnel system.

linear Fresnel solar concentrator presented in **Figure 1(b)** comprises series of linear mirror strips that tracks the sun in a single axis, in addition to concentrating the solar radiation on the receiver cavity mounted on the horizontal tower. Each mirror element is titled in such a way that usually incident solar radiation, subsequent to the reflection from the mirror element, impinges on the absorber tube as positioned along the length of the focal zone of the concentrator. The LFR system consists of an array of long parallel mirrors (termed primary mirrors) that reflects the solar rays on an absorber tube, with the possibility of including secondary reflectors in order to elevate the concentration ratio.

2.2. Plane Angle of Incidence

The angle between the mirror element and the ground was the inclination angle of the mirror element β_n. The inclination angle of the mirror in the mirror field exerts an enormous impact on the system heat collection efficiency. In accordance with the geometric relationship between mirrors of the system structure parameters and optical parameters were presented in Table 1.

When the mirror field and the sun shared the same side of the receiver, Equation (1) was utilized in order to calculate:

$$\tan\left(\alpha - 2\beta_n\right) = \frac{H}{Q_n} \tag{1}$$

When the mirror field and the sun were positioned in the receiver side, Equation (2) was put use in order to calculate:

$$\tan\left(180 - 2\beta_n - \alpha\right) = \frac{H}{Q_n} \tag{2}$$

α : incident angle of solar rays, °

Q_n : mirror distance from the center of the mirror field distance, m.

3. Mirror Field Numerical Calculation

3.1. LFR Optical Efficiency Analysis

With the use of the concepts of ray tracing approach, the Linear Fresnel solar field was presented that has been modeled as an optical-geometrical system characterized by its geometrical as well as optical characteristics for instance reflection, refraction and transmission [14]. The system is characterized by slightly curved heliostats. The solar field is modeled as a solar scene that comprises, as presented in Figure 1, two main components: The solar rays, released from the sun, taken into consideration as straight lines, Material objects with particular geometrical shapes: heliostats, absorber tube and secondary reflector. Each component is modeled in accordance with its appropriate parametric equation. Optical interactions between sun rays and components of the solar field are modeled through calculation of their intersection points, in addition to determining the new coordinates of the resulting ray [15]. In the TracePro software, the mirror field, CPC and absorption tube model were established. The mirror

Table 1. System structure parameters and optical parameters.

Project	Value	Project	Value	Project	Value
Mirror number n	10	Mirror reflectivity	0.91	Height of absorber tube H/mm	3000
Mirror width W/mm	300	Width of CPC/mm	400	Outer tube radius r^2/mm	50
Mirror length L/mm	1820	Reflectivity of CPC	0.91	Absorptivity of absorption tube	0.92
Mirror wheelbase Sn/mm	490				

substance was set to ultra white glass whereas the surface property was set to silver, and the CPC surface material together with the same characteristics was set as the mirror field; and the absorption tube material was set to aluminum. The DNI was set to 800 w/m^2, 500 × 500 of the lattice light source density. Furthermore, the ray trace pattern was presented in Figure 2.

In order to analyze the influence of latitude on the optical effectiveness of the linear Fresnel system, the numerical measurement was carried out with the similarity of the numerical measurement. With the latitude of 40.8˚, adjustment of the position of the mirror field was made in accordance with the regional latitude. Figure 3 threw light on the optical efficiency of the system with latitude 40.8˚ and latitude 0˚ with different incident angles. When the incident angle was

Figure 2. (a) System of the ray tracing and (b) Optical simulation of the compound parabolic collector.

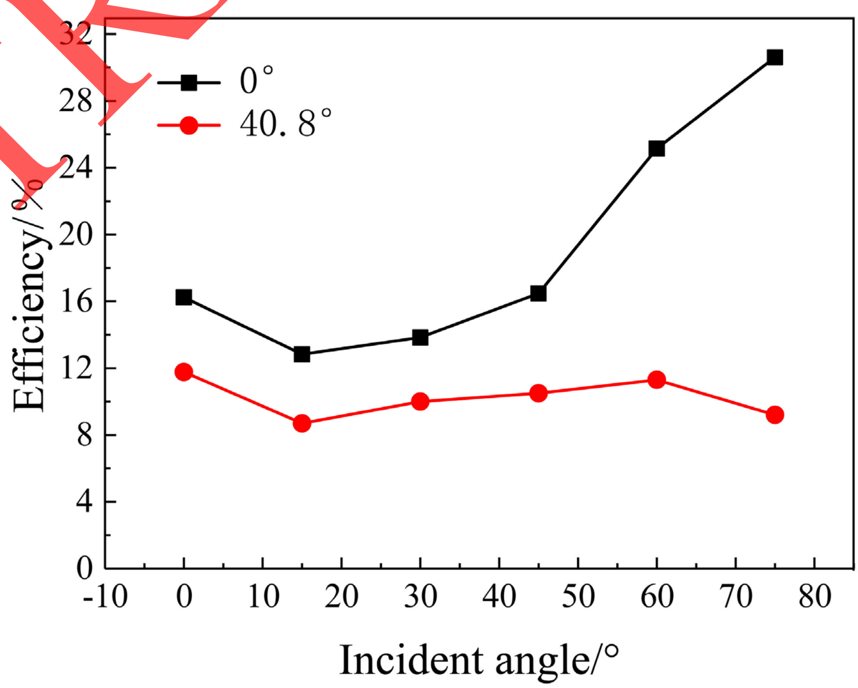

Figure 3. Variation of optical efficiency at different latitudes.

15˚, the optical efficiency amounted to be the lowest, and the loss of light in the mirror element gap was large as well, together with the formation of shadow by the CPC in the mirror element of the primary mirror field, resulting in the optical efficiency less than the efficiency of light's vertical incidence of light. As the incident angle of the light increase, it leads to the occlusion and shadow loss; when the incident angle augments to a specific degree, CPC did not generate a shadow in a mirror field. The optical loss was resulted by the gap between the mirror, and the optical efficiency of the system observed an increase. When the latitude was 40.8˚, the optical efficiency of the system amounted to be less than 0˚. As the incident angle was increased, possessing a greater difference between the two conditions, it was caused by the end of the loss. The condition was an incident angle of 75˚ together with the latitude of 40.8˚. Furthermore, the optical efficiency of the system with end of the loss and the mirror between the shadow losses firstly increased, followed by secondly decreasing.

3.2. Energy Density Distribution of the Absorber Tube

The latitude of the region exerts impact on the altitude and azimuth of the sun, in such a way that the incidence angle of the sun is different. In order to analyze the influence of latitude on the energy density of the tube wall of the absorber, analysis of the energy flux density distribution of the absorber tube wall at latitude 0 and 40.8 degrees is analyzed at the vertical incidence of the sun, as shown in respectively Figure 4 and Figure 5. As evident from the figure, representing the models due to the fact that the receiving surface are symmetrical tubular receiver, the light irradiance trend is fundamentally the same that is owed to the symmetrical position of the light paths propagation, whereby the path is fundamentally consistent. According to the analysis at latitude of 0˚, the absorption tube circumferential direction energy density distribution does not appear to be uniform, as some areas of incompetent flow distribution, part of the regional

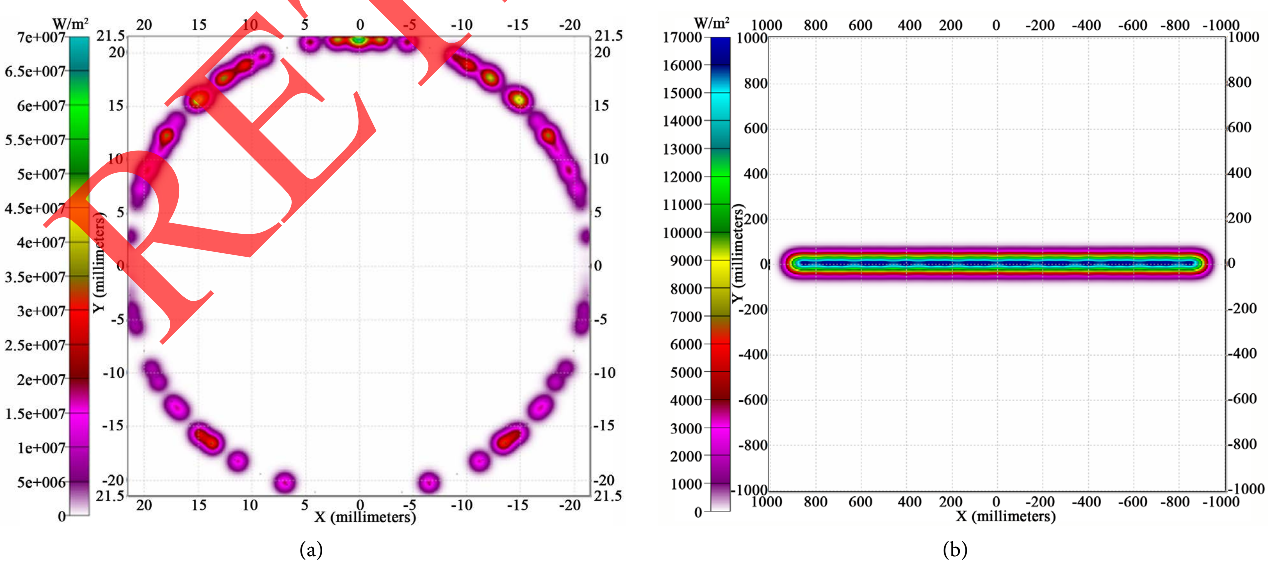

Figure 4. The receiver irradiance figure analysis at latitude 0˚ region.

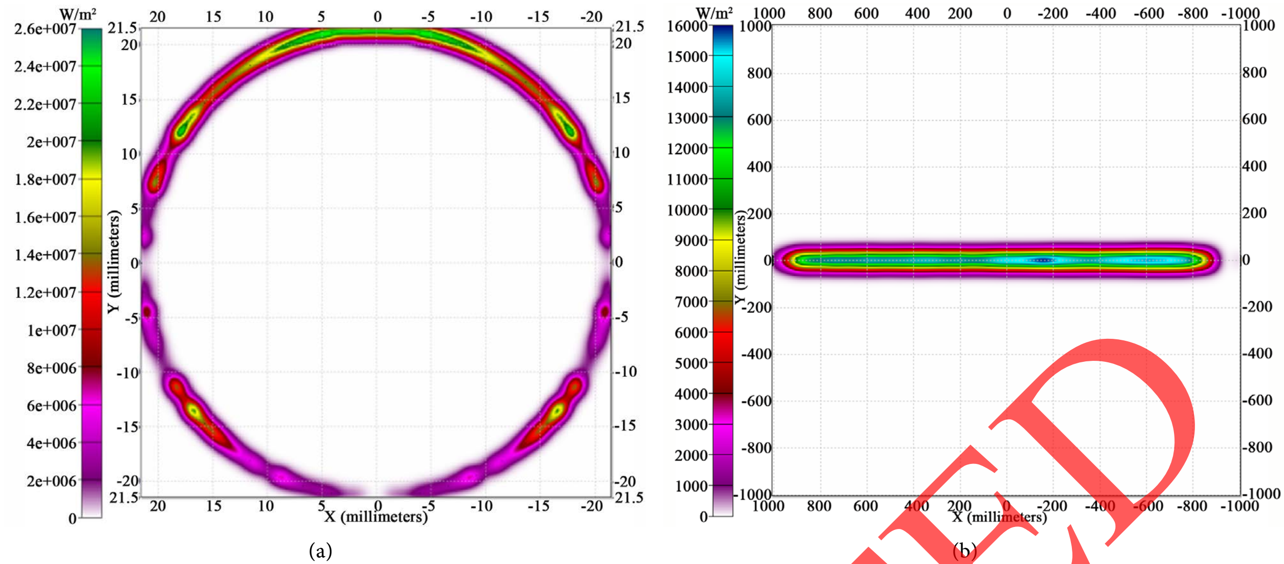

Figure 5. The receiver irradiance figure analysis at latitude 40.8˚ region.

energy density is large, and the tube length of its energy flux distribution. When the latitude is 40.8˚, it is above board that the energy flux density distribution of the absorber tube wall exhibits uniformity. On the other hand, the energy flux density direction of the tube length is reducing, and some of the pipe length is not distributed that is because of the fact that, at the same time, the latitude is 40.8˚. The angle is small that poses impact on the absorber tube wall and the tube length direction to energy flux distribution. Consequently, this energy flux is expected to result into the non-uniform temperature on every tube, and it is likely to result into two further adverse effects [16]. The first one suggests that the local high temperature is likely to accelerate the degradation of coating on tubes together with the decomposition of the heat transfer fluid. The second one is that the large thermal stress resulted by the temperature gradient may lead to undesirable distortions, in addition to damaging of the receiver, particularly as the evacuated tube put to use [17]. As evident from Figure 4 and Figure 5, the latitudinal 0˚ region is symmetrical and color distribution on the receiver does not have uniformity and the receiver is intermittent. The focus width amounted to be approximately 3 mm.

Figure 6(a) displayed the energy flux density distribution in the circumferential direction of the absorption tube. As suggested by the figure the distribution of the energy flow density of the collector tube at latitude of 40.8˚ mounted to be large and the energy flux density distribution was uniform, but the overall energy flux density was less than latitudinal area. Figure 6(b) represented the direction of the longitudinal distribution of the absorber tube; the latitude of 0˚when the longitudinal direction of the absorber tube could be distributed evenly being approximately 12,000 w/m^2. The high latitude area with the end of the loss for the absorber tube, at 1800 - 2000 mm incompetent energy flux density distribution, with the increase in tube length, energy flux density exhibited decreasing trend.

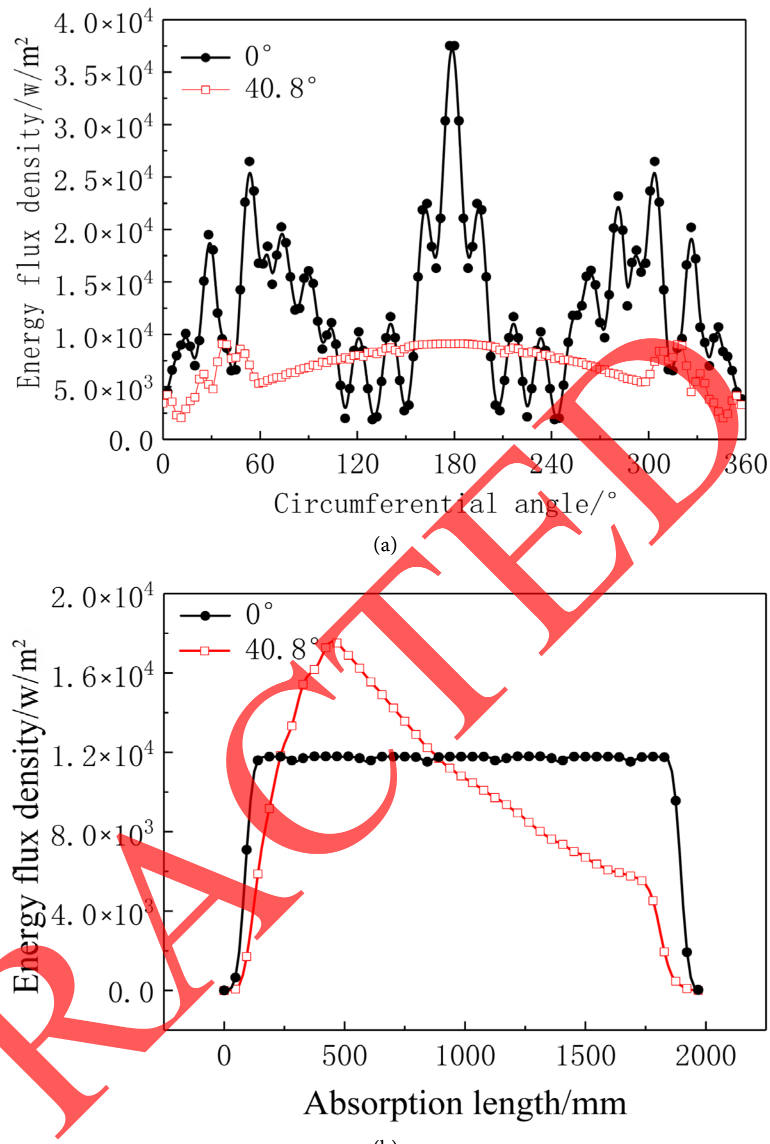

Figure 6. Energy flux density distribution of the absorber wall.

4. Thermal Performance Experiment of the System

4.1. Heat Transfer Factor of Collector

The thermal efficiency of the collector was subjected to the steady state or quasi-steady state condition, the collector energy at a specific time the effective energy income and the condenser effective area and at the same time, in order to receive the effective area of the condenser on the amount of solar radiation:

$$\eta_t = \frac{Q_n}{I \cdot A_m} = \frac{Cq_m\left(t_{\text{out}} - t_{\text{in}}\right)}{I \cdot A_m} \tag{3}$$

In accordance with the energy balance equation of the absorber:

$$\eta_t = \frac{Q_n}{I \cdot A_m} = \frac{Q_{\text{total}} - Q_{\text{loss}}}{I \cdot A_m} = \eta_0 - \frac{U_L\left(t_r - t_{env}\right)}{I \cdot A_m} \tag{4}$$

Q_{total} suggested the total heat of the suction absorber tube, Q_{loss} indicated the heat loss of the absorber tube, U_L represented the heat loss coefficient, t_r implied the absorber tube surface temperature, t_{env} depicted the ambient temperature.

The absorber constituted of a CPC and a vacuum heat collector, together with being was higher than the reflector 4 m. The surface temperature was not easily calculated. Moreover, the inlet and outlet temperature of the working fluid could be attained with the help of the temperature sensor. That is the reason that the heat transfer factor F_R was introduced for the purpose of representing the heat Collector surface temperature for the working fluid inlet temperature when the heat ratio, and the instantaneous collector efficiency expression were rewritten as:

$$\eta_t = F_R - \frac{F_R U_L}{A_m} \cdot \frac{t_{in} - t_{out}}{I} \tag{5}$$

If F_R, U_L and theoretical optical efficiency were constant, the instantaneous collector efficiency modified with the normalized temperature difference as a function. All through the experiment, F_R appeared to be a weak function of U_L, whereas U_L was a function of wind speed as well as operating temperature. Linear equation suitable to the thermal efficiency of the collector was a very good approximation, that made use of the efficiency curve and the Y-axis intercept for the purpose of estimating the actual optical efficiency. Furthermore, the slope can be applied in order to estimate the total heat loss coefficient of the collector.

4.2. Measurement of System Instantaneous Heat Collection Efficiency

Combined with the cold season in the spring area with larger sand amounts, the sun height angle is small, and the ambient temperature was low, as per the experiment in Inner Mongolia Hohhot (111˚E, 40.8˚N) outdoors. The weather tests showed clear, with no continuous wind direction, and the working fluid flow was 0.2 m/s. The pipeline cycle heat collection experiment, was performed for the purpose of precisely analyzing the system instantaneous thermal efficiency of the system with the normalized temperature difference (T^*) through the selection of 11: 30-13: 30 data for analysis, measured data has been presented in Figure 7.

$$T^* = \frac{T_i - T_{env}}{I} \tag{6}$$

According to the above mentioned method of calculation, the experimental data processing from Figure 8 revealed that the refrigerant inlet temperature was 60˚C, 70˚C and 73˚C, in correspondence with the instantaneous thermal efficiency of 58%, 56% and 49%. In accordance with the empirical data, the instantaneous thermal efficiency equation of the collector by the least squares fitting was:

$$\eta_t = 0.68 - 3.16T^* \tag{7}$$

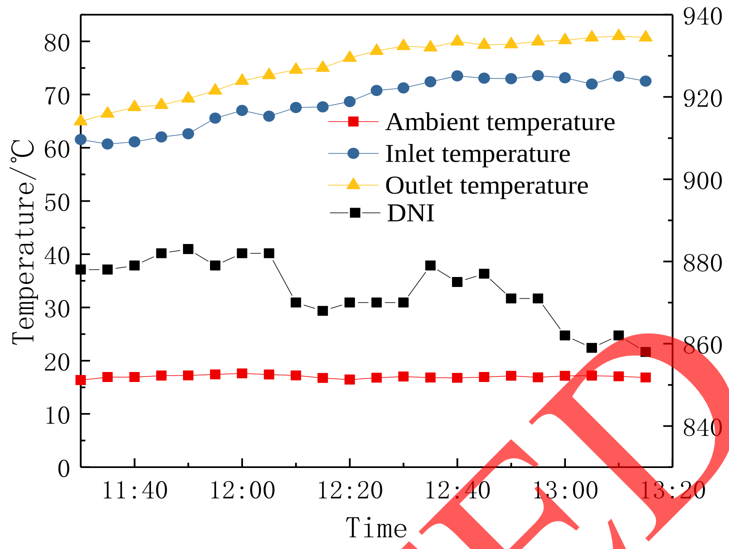

Figure 7. Measured data for linear Fresnel reflector system.

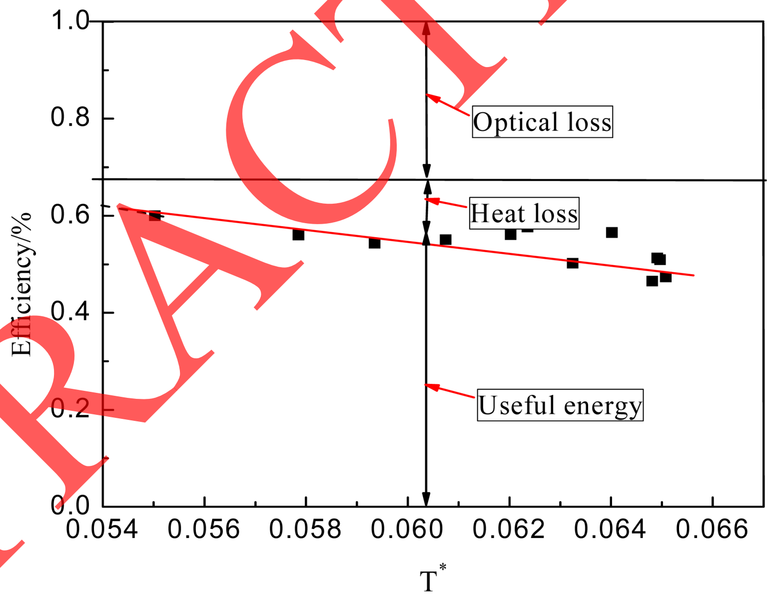

Figure 8. The efficient curve of collecting system.

The key factors that exert impact on the efficiency of the linear Fresnel collector include the inlet temperature, ambient temperature and direct solar irradiance. The inlet and outlet temperature of the working fluid is slowly and steadily elevated all through the experiment, and the temperature difference between the inlet and outlet amounts to be 5˚C - 8˚C. All through the test, the oil pump was in stable running state, and its mass flow rate was maintained at 0.22 kg/s. A prediction is made here that the temperature of the outlet heat transfer oil generated by the autumn will embrace great improvement because of the improvement of collector optical efficiency together with the enhancement of direct radiation. As evident from in Equation (7), we can observe an intercepted efficiency of 68%, with the data selected in this article for the period of no end loss.

As suggested by the change trend of the system heat collection efficiency in Figure 7, it can be observed that the smaller the difference between the inlet temperature and the ambient temperature, the greater the direct solar irradiance, and the higher the collector efficiency. Figure 8 revealed that the total optical loss of the system accounted for 32% of total solar radiation, which enhanced the performance of the absorber at the same time. The system structure was optimized, decreased for the spacing of the mirror, and reduced in the optical loss. While a heat loss of the system showed a reduction with the improvement in the inlet temperature of working fluid, so the system thermal efficiency was reduced. The thermal loss coefficient of the linear Fresnel system mounted to be 3.16 $W/m^2 \cdot {}^\circ C$, and the heat loss coefficient of the whole system, included the heat loss of vacuum tubes, pipes, tanks and other systems. In the cold region, the linear Fresnel concentrator system is quite essential for the reduction of the optical loss while maintaining the system's thermal insulation.

5. Conclusions

In this paper, we primarily performed the comparison of the optical efficiency of the linear Fresnel system subjected to different latitudes, and obtained the energy flux density distribution of the absorber tube. On the second place, the thermal transfer factor was put to use for the purpose of the linear Fresnel experimental system, in addition to analyzing the system instantaneous thermal efficiency changes, attaining some conclusions:

1) The optical efficiency of the high latitudes amounted to be smaller in comparison with that of the low latitudes, and with the increased in the incident angle of the sun, the difference between the two conditions appeared to be larger, owing to the end loss effect.

2) The thermal loss coefficient of the linear Fresnel system was 3.16 $W/m^2 \cdot {}^\circ C$, which included the vacuum loss of vacuum tube, pipeline, oil tank etc. This value will follow the function of enhancing the thermal insulation performance of the system.

3) The optical loss of the system accounts for 32% of the total solar radiation, which could bring for a basis for the subsequent optimization of the system structure.

In conclusion, the LFR system simulation analysis as well as experimental test principle in different latitudes is both correct and reliable that provides a good reference for the optimal arrangement of linear Fresnel collector system in the cold region. TracePro software is capable of simulating and analyzing the optical performance of the collector system in different latitudes. Furthermore, there is the feedback to the system parameter design that provides some theoretical guidance for the application of LFR system in the cold region.

Acknowledgements

This work was financially supported by Inner Mongolia Graduate Scientific Research Innovation Project (2016).

References

[1] Montes, M.J., Rubbia, C., Abbas, R. and Martínez-Val, J.M. (2014) A Comparative Analysis of Configurations of Linear Fresnel Collectors for Concentrating Solar Power. *Energy*, **73**, 192-203. https://doi.org/10.1016/j.energy.2014.06.010

[2] Zhu, J. and Huang, H. (2014) Design and Thermal Performances of Semi-Parabolic Linear Fresnel Reflector Solar Concentration Collector. *Energy Conversion & Management*, **77**, 733-737. https://doi.org/10.1016/j.enconman.2013.10.015

[3] Mills, D.R. and Morrison, G.L. (2000) Compact Linear Fresnel Reflector Solar Thermal Power Plants. *Solar Energy*, **68**, 263-283. https://doi.org/10.1016/S0038-092X(99)00068-7

[4] Mills, D.R., Morrison, G.L., Pye, J. and Le Lièvre, P. (2006) Multi-Tower Line Focus Fresnel Array Project. *Journal of Solar Energy Engineering*, **128**, 118-121. https://doi.org/10.1115/1.2148971

[5] Schenk, H., Hirsch, T., Feldhoff, J.F. and Wittmann, M. (2012) Energetic Comparison of Linear Fresnel and Parabolic Trough Collector Systems. *Journal of Solar Energy Engineering*, **136**, 333-344. https://doi.org/10.1115/ES2012-91109

[6] Abbas, R., Munoz, J., and Martínez-Val, J.M. (2012) Steady-State Thermal Analysis of an Innovative Receiver for Linear Fresnel Reflectors. *Applied Energy*, **92**, 503-515. https://doi.org/10.1016/j.apenergy.2011.11.070

[7] Abbas, R., Montes, M.J., Rovira, A., *et al.* (2016) Parabolic Trough Collector or Linear Fresnel Collector: A Comparison of Optical Features Including Thermal Quality Based on Commercial Solution. *Solar Energy*, **124**, 198-215. https://doi.org/10.1016/j.solener.2015.11.039

[8] Pye, J.D., Morrison, G.L., Behnia, M. and Mills, D.R. (2003) Modelling of Cavity Receiver Heat Transfer for the Compact Linear Fresnel Reflector. ISES Solar World Congress, Sweden.

[9] Abbas, R. and Martínez-Val, J.M. (2015) Analytic Optical Design of Linear Fresnel Collectors with Variable Widths and Shifts of Mirrors. *Renewable Energy*, **75**, 81-92. https://doi.org/10.1016/j.renene.2014.09.029

[10] Zhu, G., Wendelin, T., Wagner, M.J. and Kutscher, C. (2014) History, Current State, and Future of Linear Fresnel Concentrating Solar Collectors. *Solar Energy*, **103**, 639-652. https://doi.org/10.1016/j.solener.2013.05.021

[11] Grena, R. and Tarquini, P. (2011) Solar Linear Fresnel Collector Using Molten Nitrates as Heat Transfer Fluid. *Energy*, **36**, 1048-1056. https://doi.org/10.1016/j.energy.2010.12.003

[12] Qiu, Y., He, Y.L., *et al.* (2016) A Comprehensive Model for Optical and Thermal Characterization of a Linear Fresnel Solar Reflector with a Trapezoidal Cavity Receiver. *Renew Energy*, **97**, 129-144. https://doi.org/10.1016/j.renene.2016.05.065

[13] Qiu, Y., He, Y.L., Cheng, Z.D., *et al.* (2015) Study on Optical and Thermal Performance of a Linear Fresnel Solar Reflector Using Molten Salt as HTF with MCRT and FVM Methods. *Applied Energy*, **146**, 162-173. https://doi.org/10.1016/j.apenergy.2015.01.135

[14] Zhu, G. (2013) Development of an Analytical Optical Method for Linear Fresnel Collectors. *Solar Energy*, **94**, 240-252. https://doi.org/10.1016/j.solener.2013.05.003

[15] Roccia, J.P., Paulin, M. and Coustet, C. (2013) Hybrid CPU/GPU KD-Tree Construction for Versatile Ray Tracing. *Eurographics Symposium on Rendering*.

[16] Qiu, Y., He, Y.L., Liang, Q., *et al.* (2016) A MCRT-FVM Simulation Method for the

Coupled Photo-Thermal Conversion Process in a Linear Fresnel Reflector Solar Collector. *Journal of Engineering Thermophysics*, **37**, 2142-2149.

[17] Eck, M., Uhlig, R., Mertins, M., Häberle, A. and Lerchenmüller, H. (2007) Thermal Load of Direct Steam-Generating Absorber Tubes with Large Diameter in Horizontal Linear Fresnel Collectors. *Heat Transfer Engineering*, **28**, 42-48. https://doi.org/10.1080/01457630600985659